ASII-GW („Automatic Satellite Image Interpretation – Gravity Waves“)

Alexander Jann, DMM/VHMOD/Remote-Sensing

Nowcasting-SAF User Workshop, 10-12 March 2020, Madrid

ZAMG
Zentralanstalt für Meteorologie und Geodynamik

Potential motivation for gravity wave search

From Keller et al. (2015)

ASII-GW: Motivation

- Gravity waves may become unstable, eventually resulting in the notorious “clear-air turbulence”
- Often reflected (only) in the WV image as a grating pattern (alternating bright and dark stripes)
- The fluctuations are fairly weak, however, so it is not easy to spot them in standard image visualizations
- Therefore: automatic pattern recognition, adapting models from the 1990’s (that tried to mimic the response of visual neurons of monkeys in case of spotting parallel lines)

ZAMG Zentralanstalt für Meteorologie und Geodynamik

The challenge - search for gravity wave ripples in WV7.3

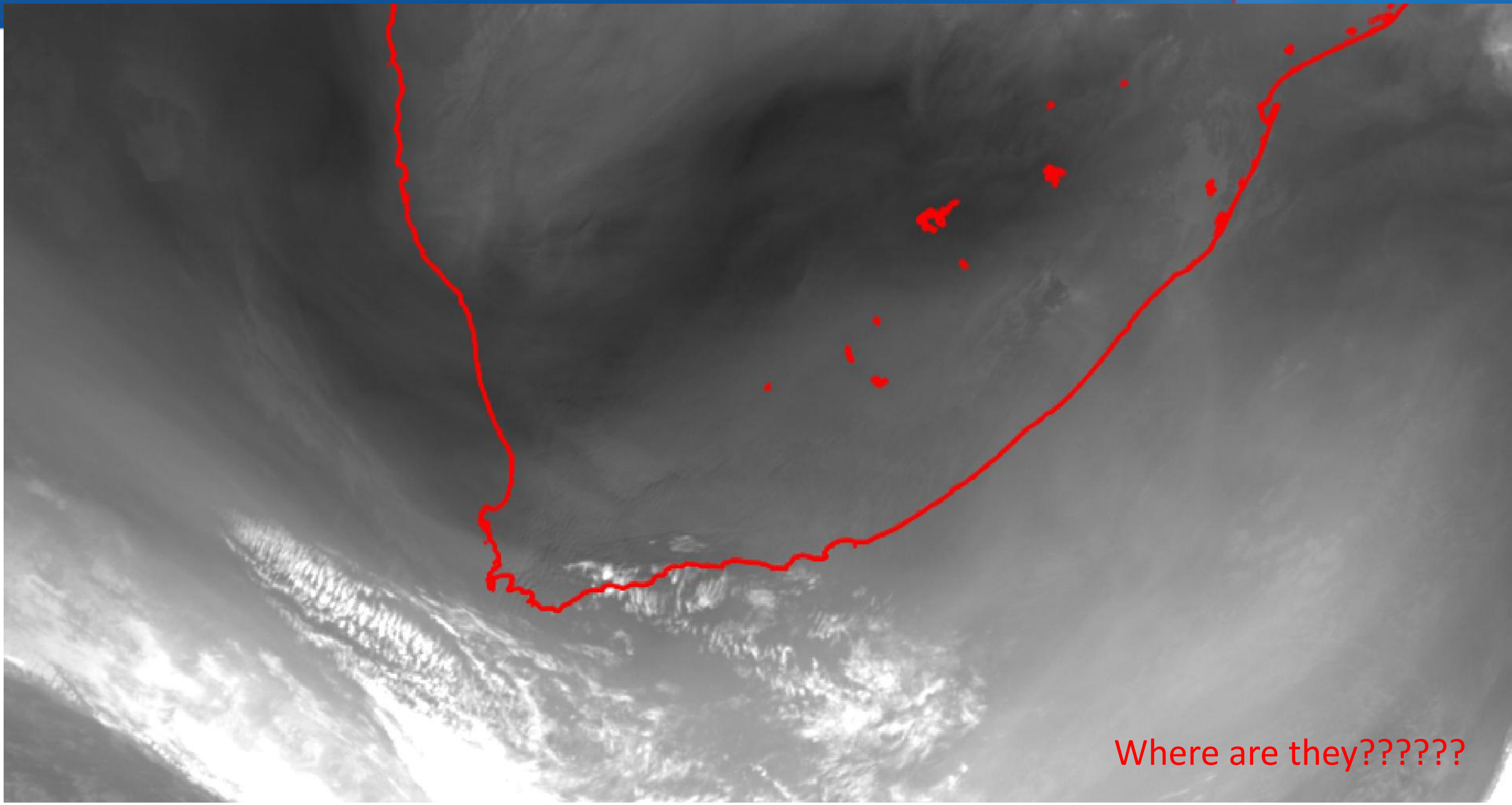

(Southernmost part of Africa, (29 June 2017, 1400 UTC)

ZAMG
Zentralanstalt für Meteorologie und Geodynamik

Algorithm, step 1: Apply a Gabor filter onto the WV7.3 image

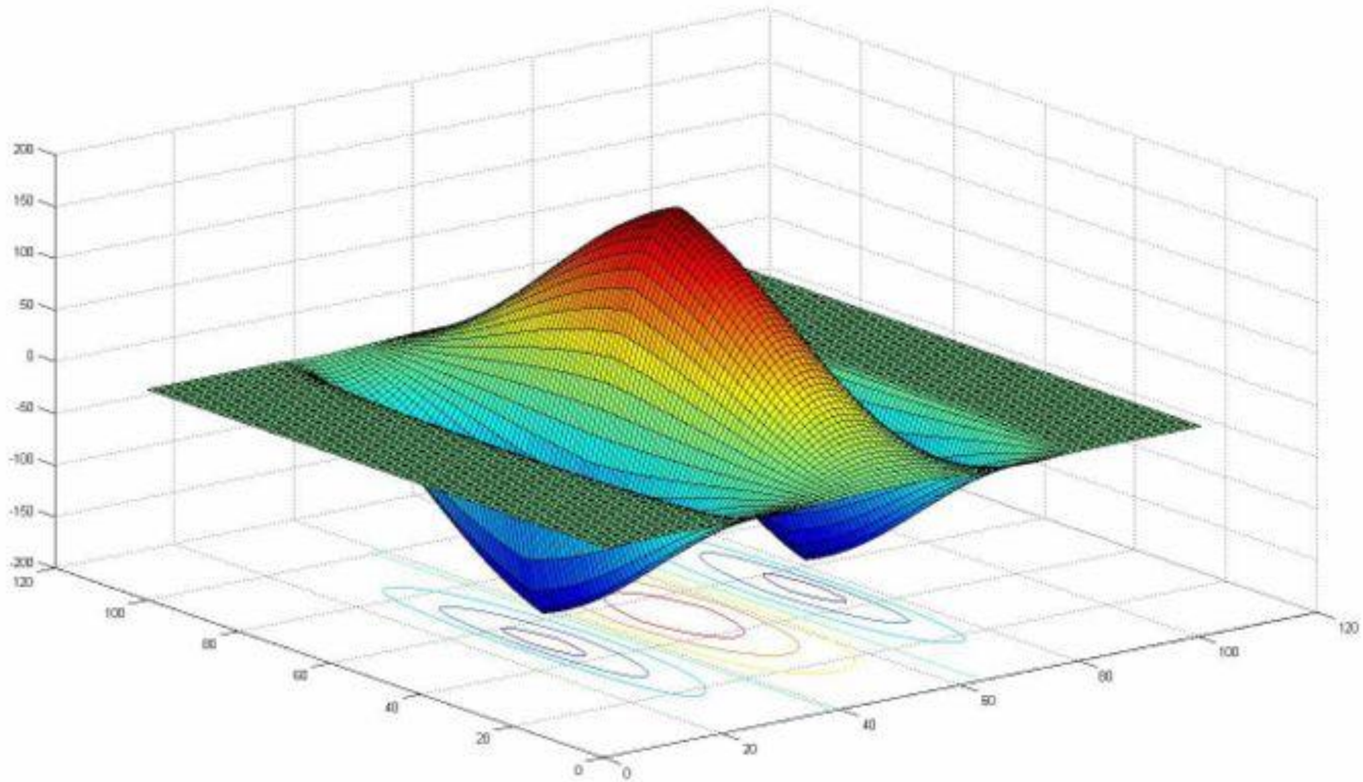

Algorithm, step 2: Apply the grating cell operator

Verifying that we have alternating positive and negative Gabor filter responses of comparable magnitude

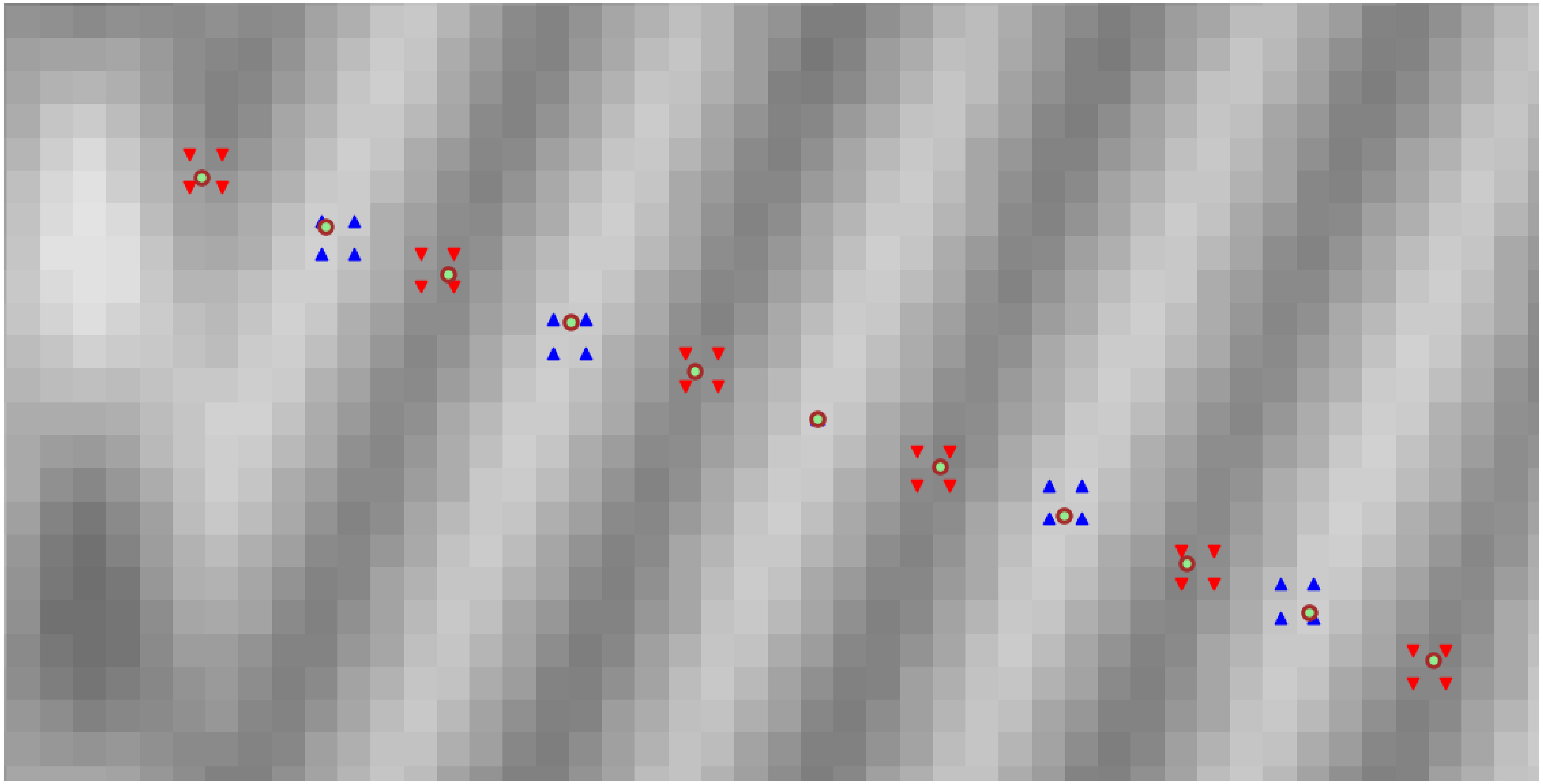

The necessity of the grating cell operator (from Petkov and Kruizinga, 1997)

a) image to be analysed
b) the Gabor filter alone (as well as probably any other operator describing brightness variability)
c) Gabor filter plus subsequent grating cell operator

a b c

ASII-GW: Method

- The Gabor filter / grating cell operator is run for several orientations and wavelengths
- The signal density is translated into a probability-of-occurrence (0-100%, for every pixel)
- More algorithmic details can be found in Jann (2017)
- After the automatic detection directs to the right areas, one can achieve displays like the following one (highlighting the gravity wave-induced WV patterns through some tailored image enhancement!):

MSG-1/IODC analysis, 29 June 2017, 1400 UTC

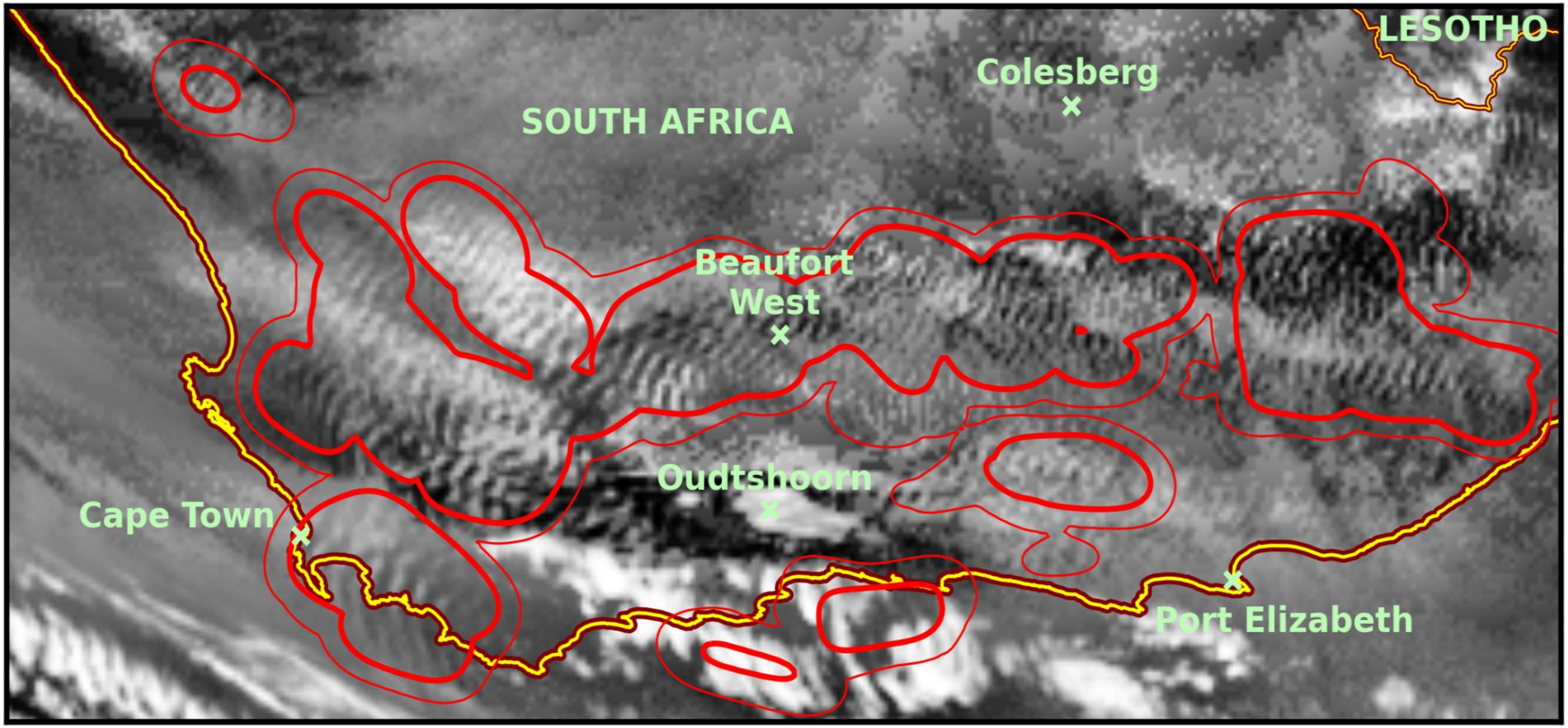

(Red isolines refer to the signal density of the ASII-GW pattern recognition algorithm)

An actual ASII-GW probabilities output

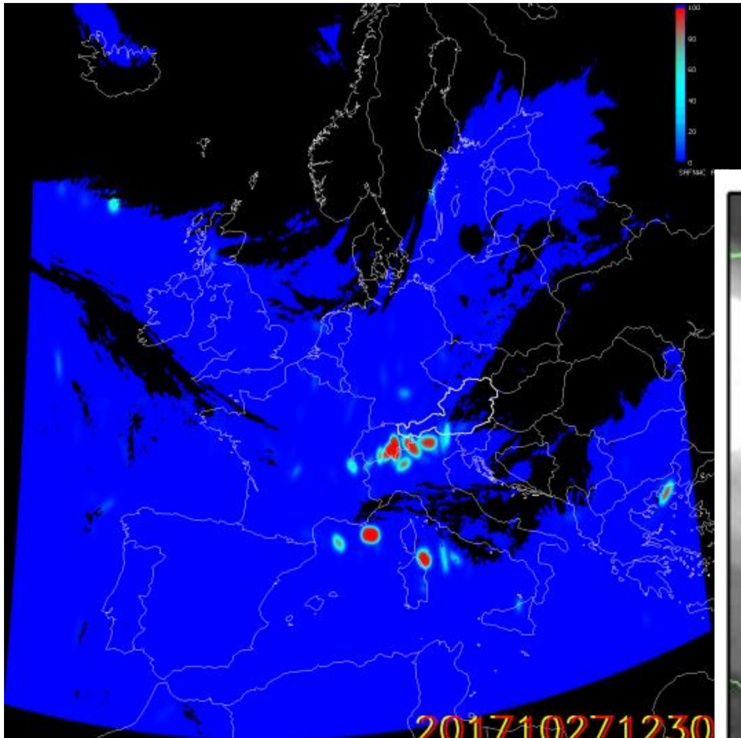

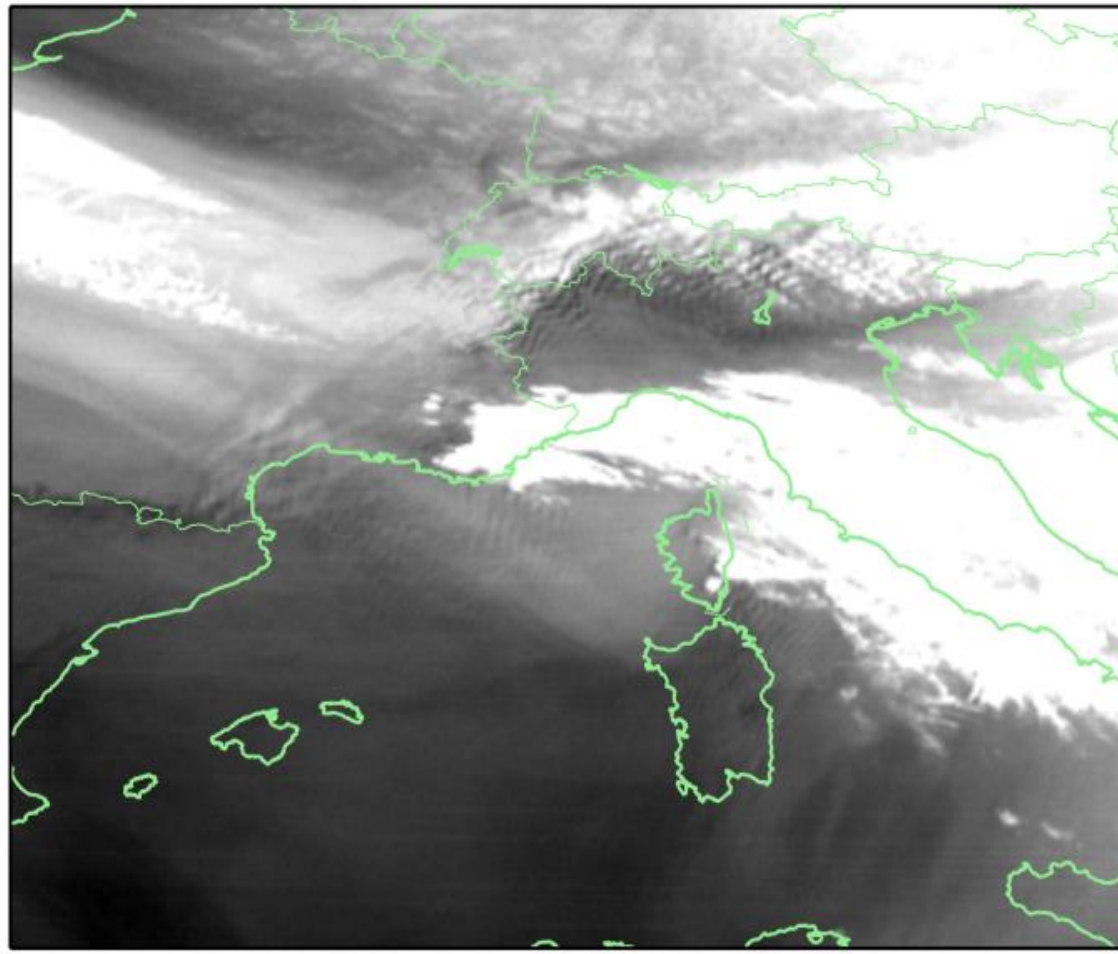

Geodynamik

What ASII-GW does (and does not) for you

- It does NOT claim to detect areas of turbulence
  - there are other mechanisms leading to turbulence
  - nor is any gravity wave necessarily breaking into turbulence
- It does NOT claim to detect all gravity waves
  - they are not necessarily in the right height to become visible in WV7.3
  - MSG SEVIRI‘s spatial resolution is not high enough to capture them all
    - warning from Wimmers et al. (2018), based on looking at AHI/ABI: *„With such an abundance of gravity wave activity suddenly in view in a geostationary image, the new challenge for forecasters is no longer where to find gravity waves because of their potential for turbulence, but rather how to distinguish turbulence-generating gravity waves from more common, benign gravity waves.”*
- **<u>Its value (today) is to obviate the tedious subjective search for the grating patterns in WV7.3</u>**
- Scientifically validated for MSG, one campaign carried out for Himawari as well; technically capable of handling GOES-R input

About temporal coherence…

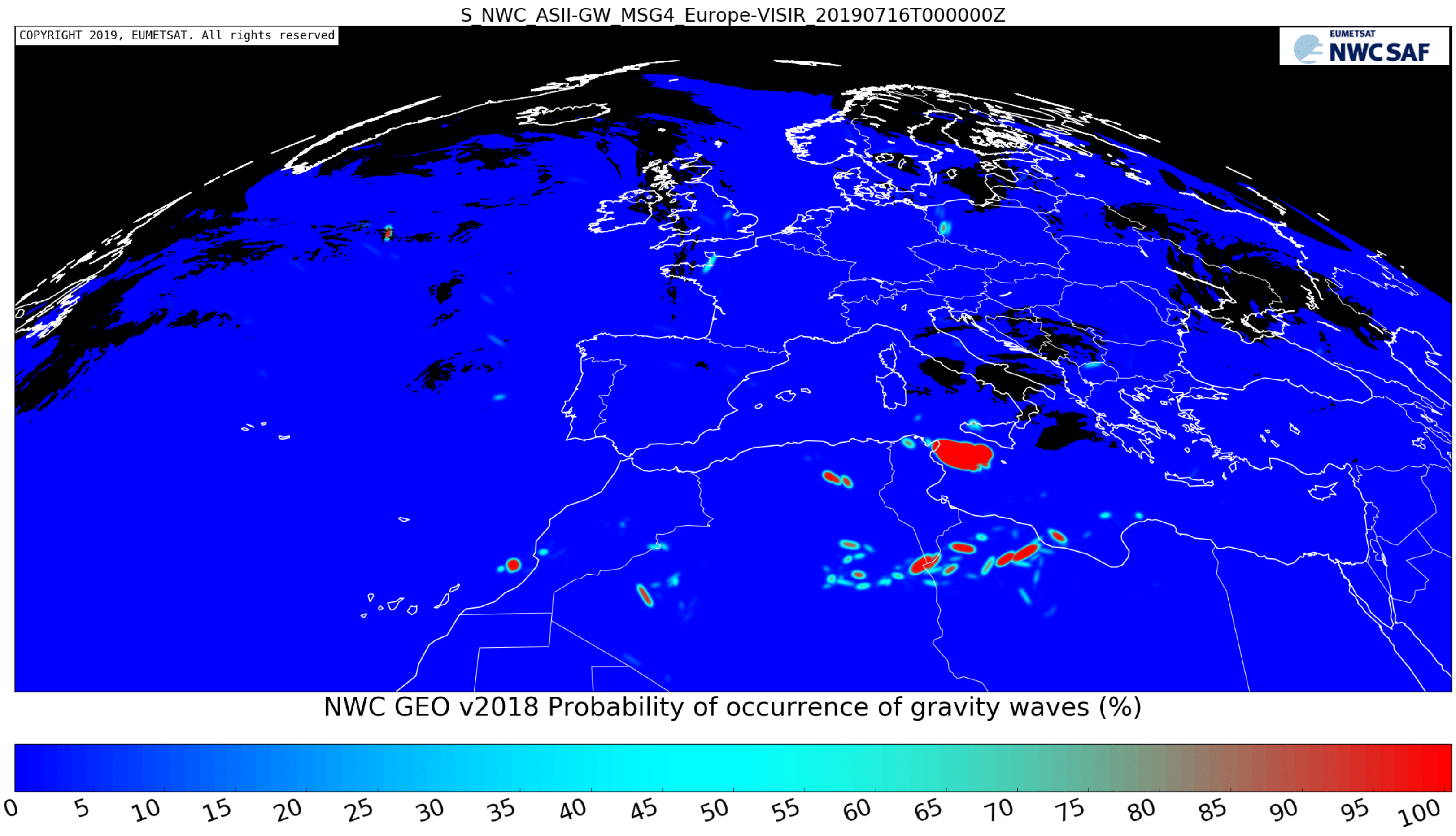

S_NWC_ASII-GW_MSG4_Europe-VISIR_20190716T001500Z

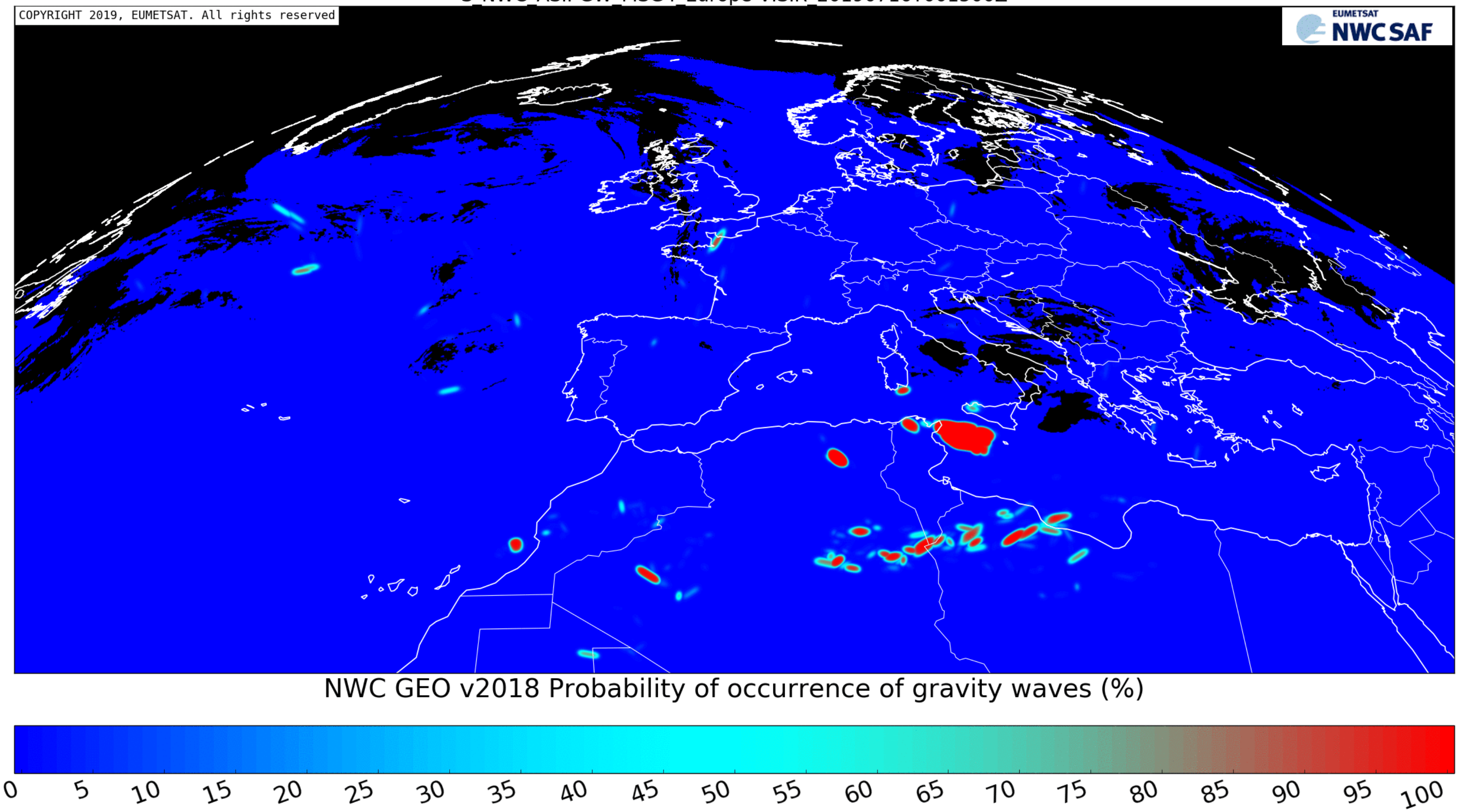

NWC GEO v2018 Probability of occurrence of gravity waves (%)

ZAMG Zentralanstalt für Meteorologie und Geodynamik

S_NWC_ASII-GW_MSG4_Europe-VISIR_20190716T003000Z

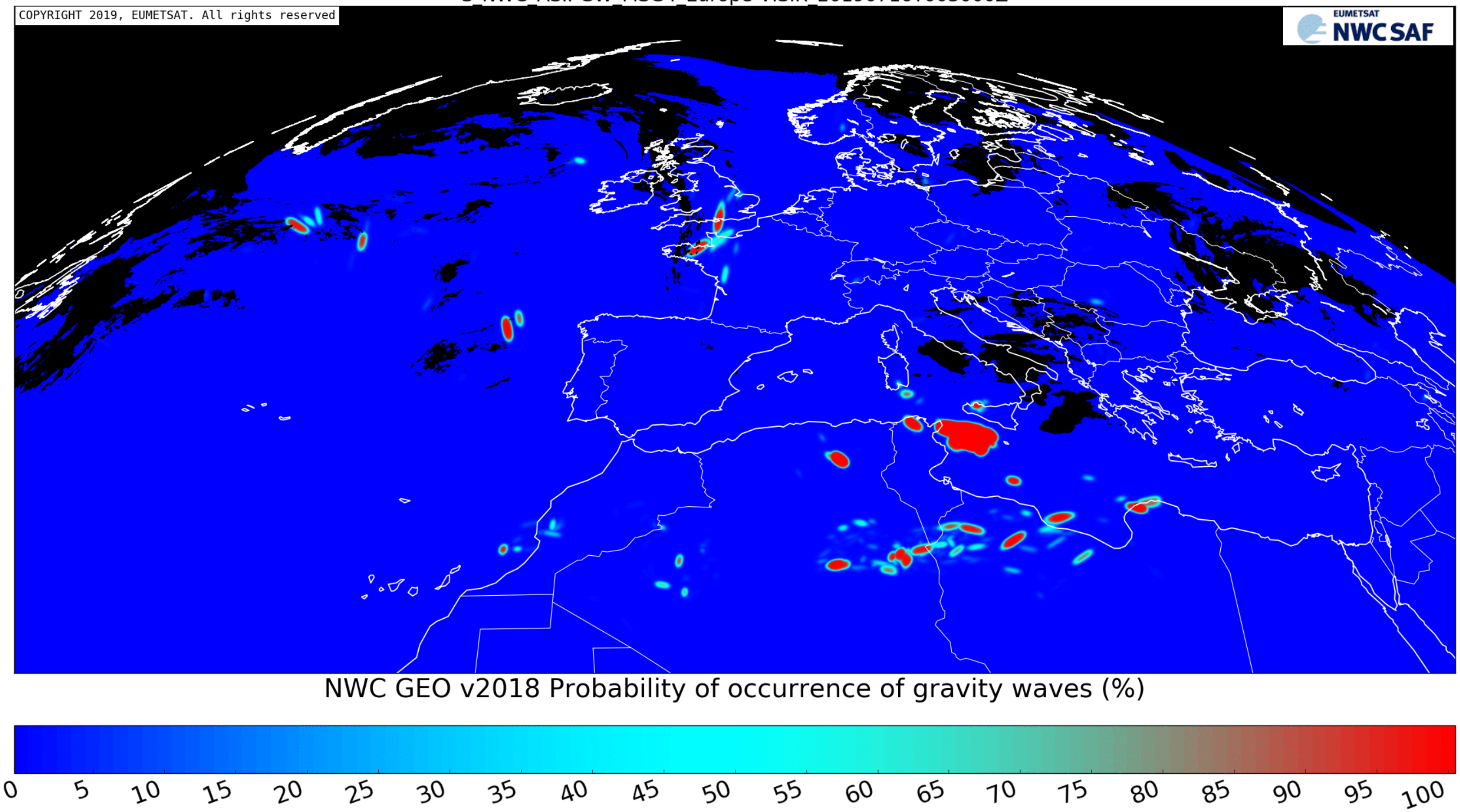

ZAMG
Zentralanstalt für Meteorologie und Geodynamik

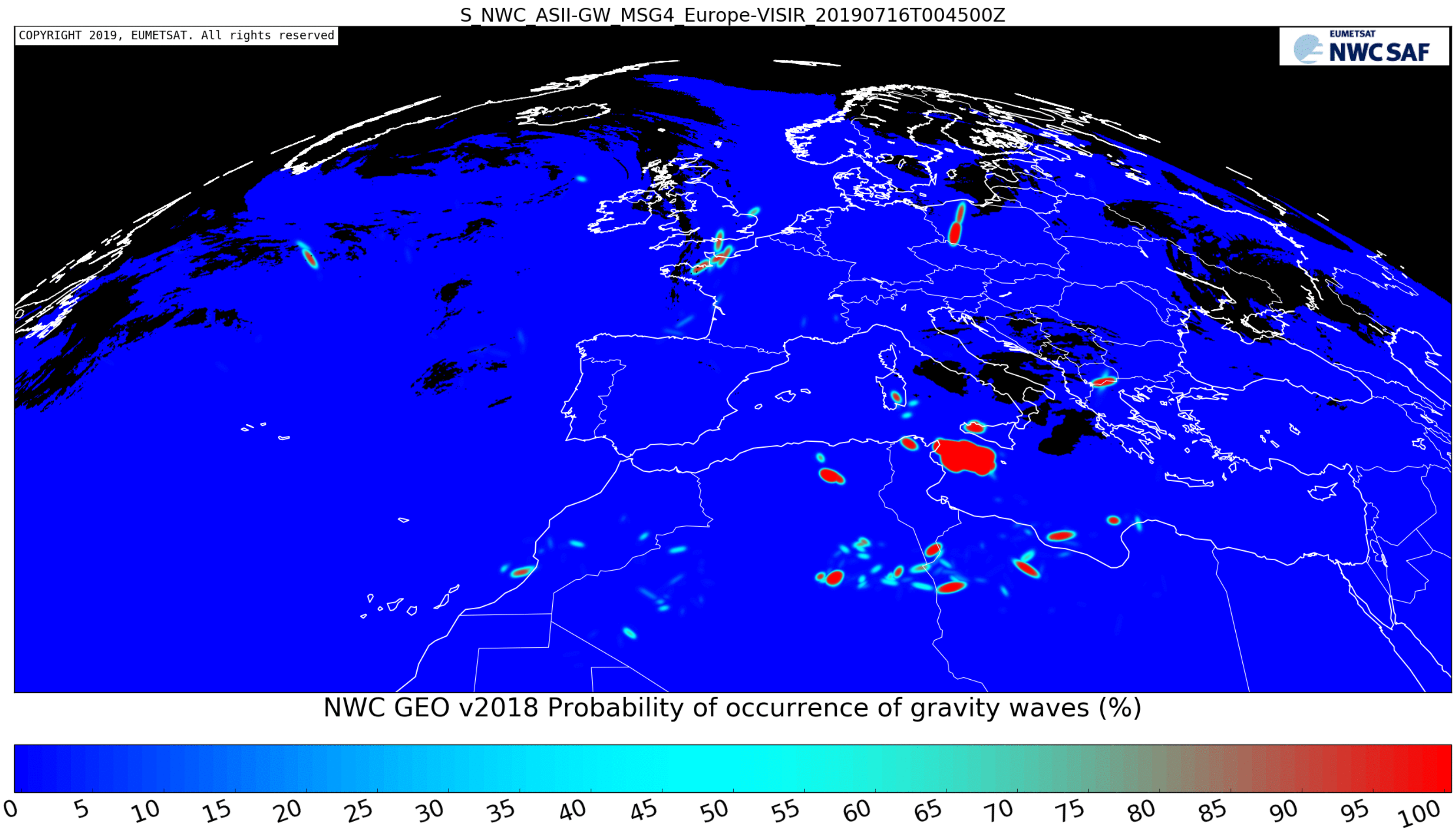
S_NWC_ASII-GW_MSG4_Europe-VISIR_20190716T004500Z
COPYRIGHT 2019, EUMETSAT. All rights reserved
EUMETSAT NWC SAF
NWC GEO v2018 Probability of occurrence of gravity waves (%)
0 5 10 15 20 25 30 35 40 45 50 55 60 65 70 75 80 85 90 95 100

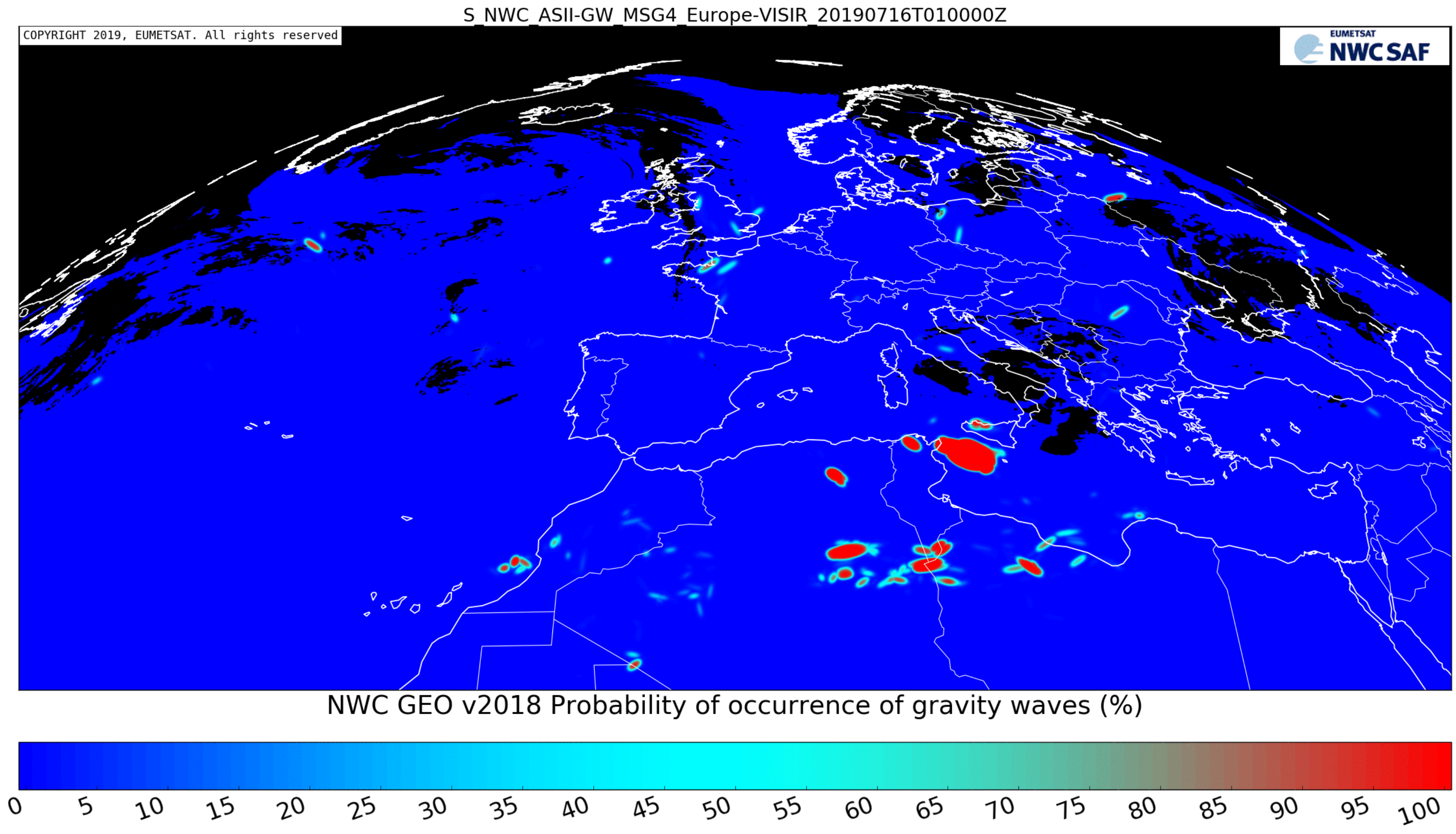
S_NWC_ASII-GW_MSG4_Europe-VISIR_20190716T010000Z
COPYRIGHT 2019, EUMETSAT. All rights reserved
EUMETSAT
NWC SAF
NWC GEO v2018 Probability of occurrence of gravity waves (%)
0
5
10
15
20
25
30
35
40
45
50
55
60
65
70
75
80
85
90
95
100

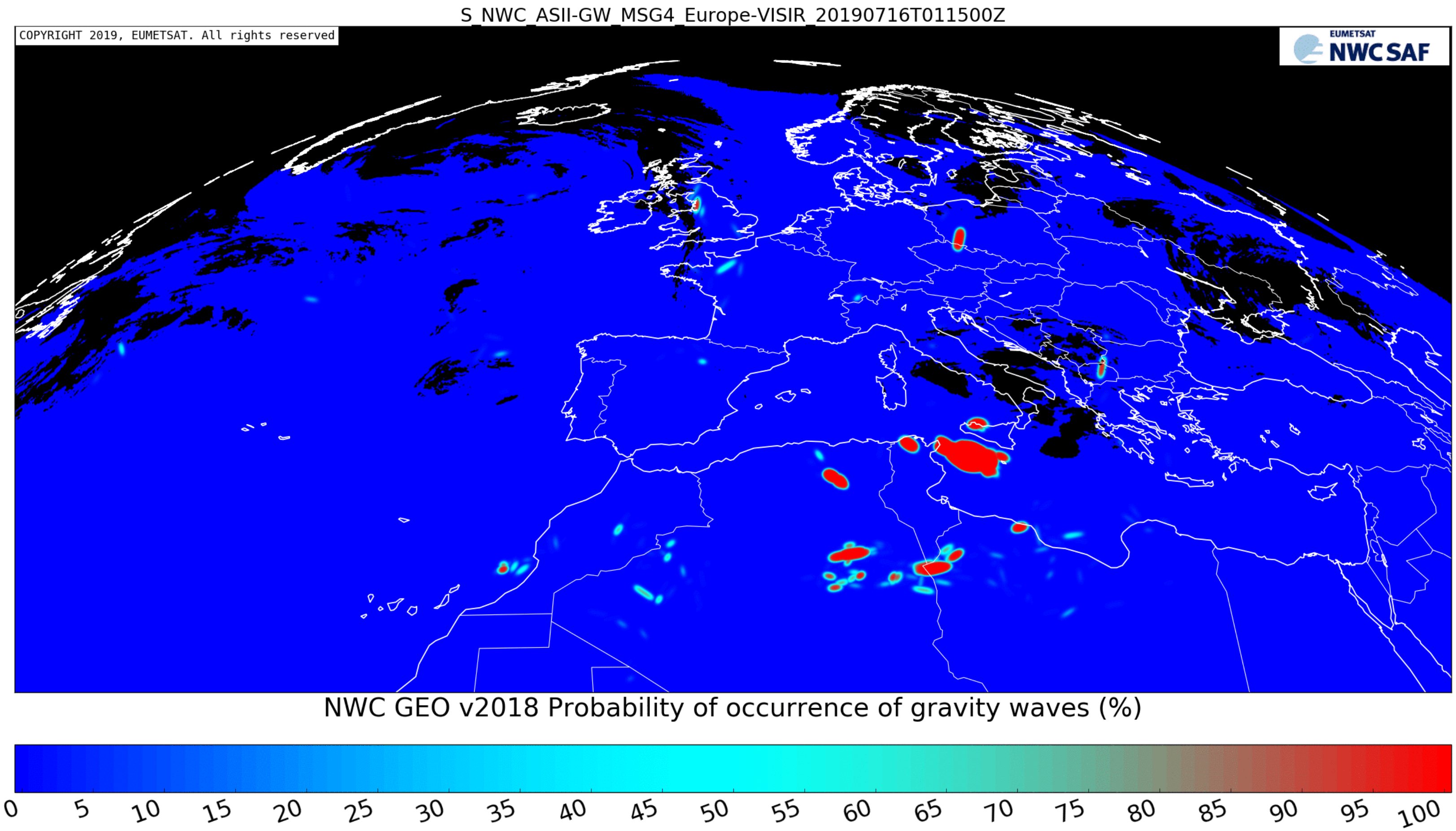
S_NWC_ASII-GW_MSG4_Europe-VISIR_20190716T011500Z
COPYRIGHT 2019, EUMETSAT. All rights reserved
EUMETSAT
NWC SAF
NWC GEO v2018 Probability of occurrence of gravity waves (%)
0 5 10 15 20 25 30 35 40 45 50 55 60 65 70 75 80 85 90 95 100

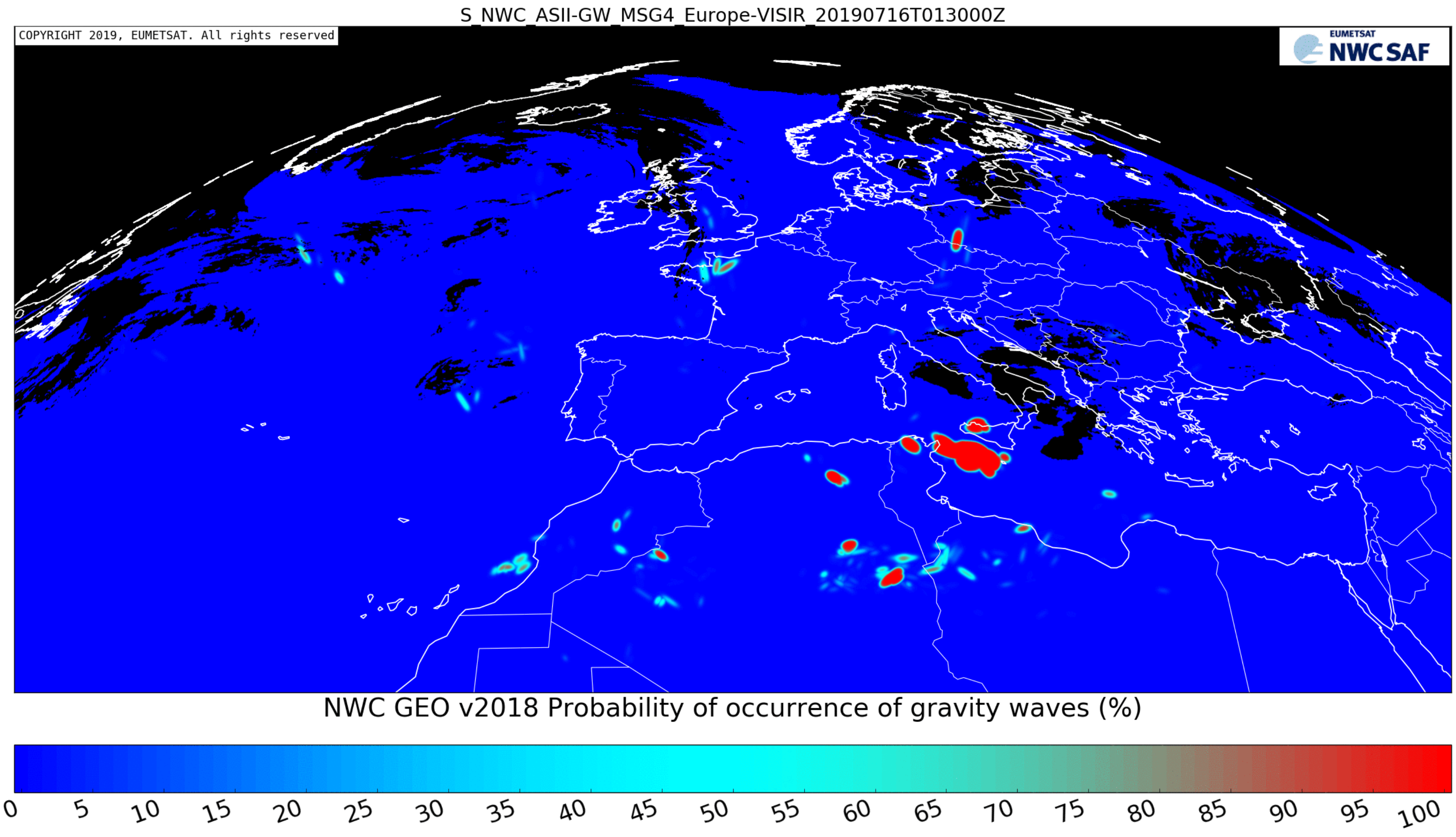
S_NWC_ASII-GW_MSG4_Europe-VISIR_20190716T013000Z
COPYRIGHT 2019, EUMETSAT. All rights reserved
EUMETSAT
NWC SAF
NWC GEO v2018 Probability of occurrence of gravity waves (%)
0 5 10 15 20 25 30 35 40 45 50 55 60 65 70 75 80 85 90 95 100

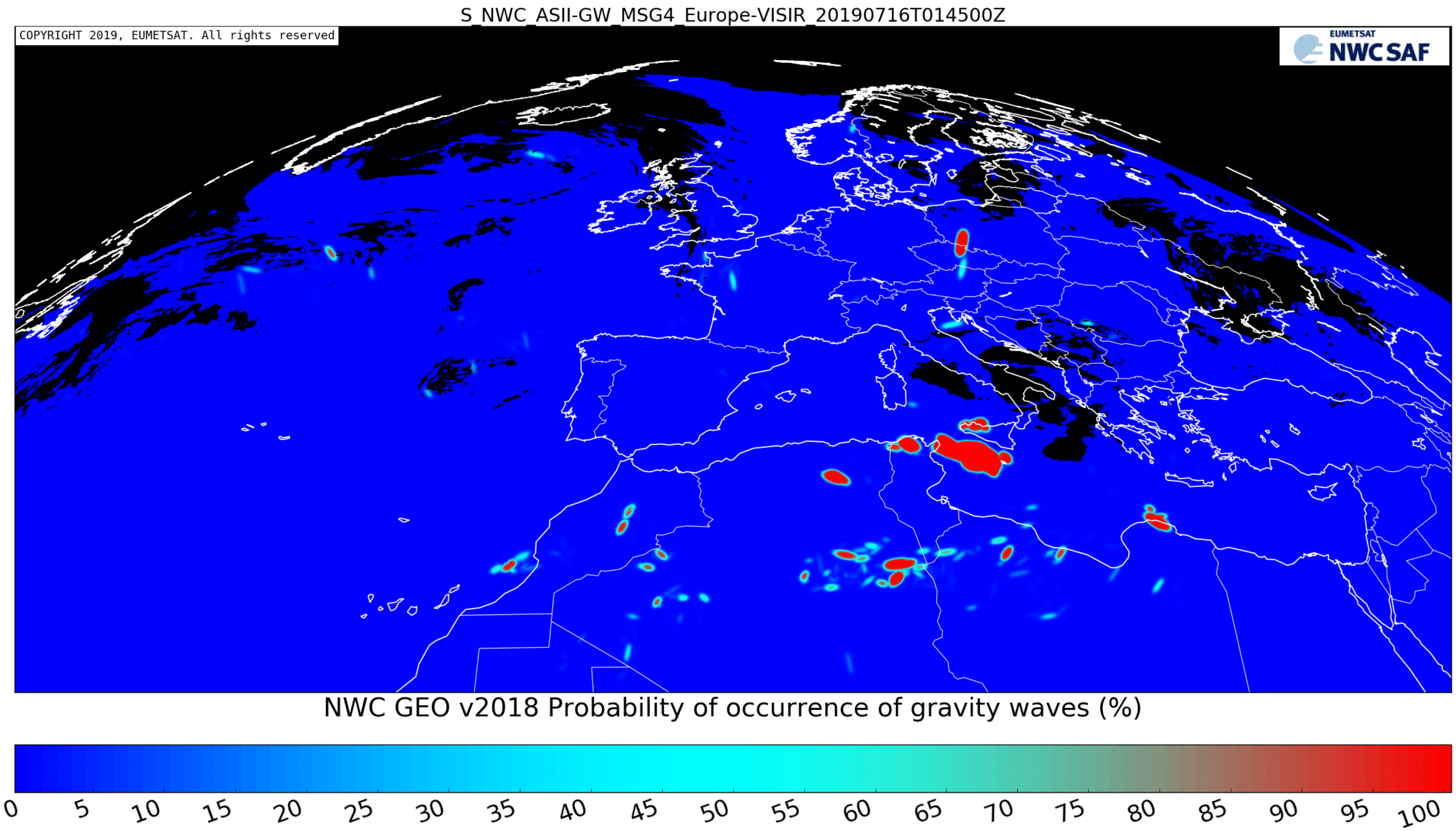
S_NWC_ASII-GW_MSG4_Europe-VISIR_20190716T014500Z
COPYRIGHT 2019, EUMETSAT. All rights reserved
EUMETSAT
NWC SAF
NWC GEO v2018 Probability of occurrence of gravity waves (%)
0
5
10
15
20
25
30
35
40
45
50
55
60
65
70
75
80
85
90
95
100

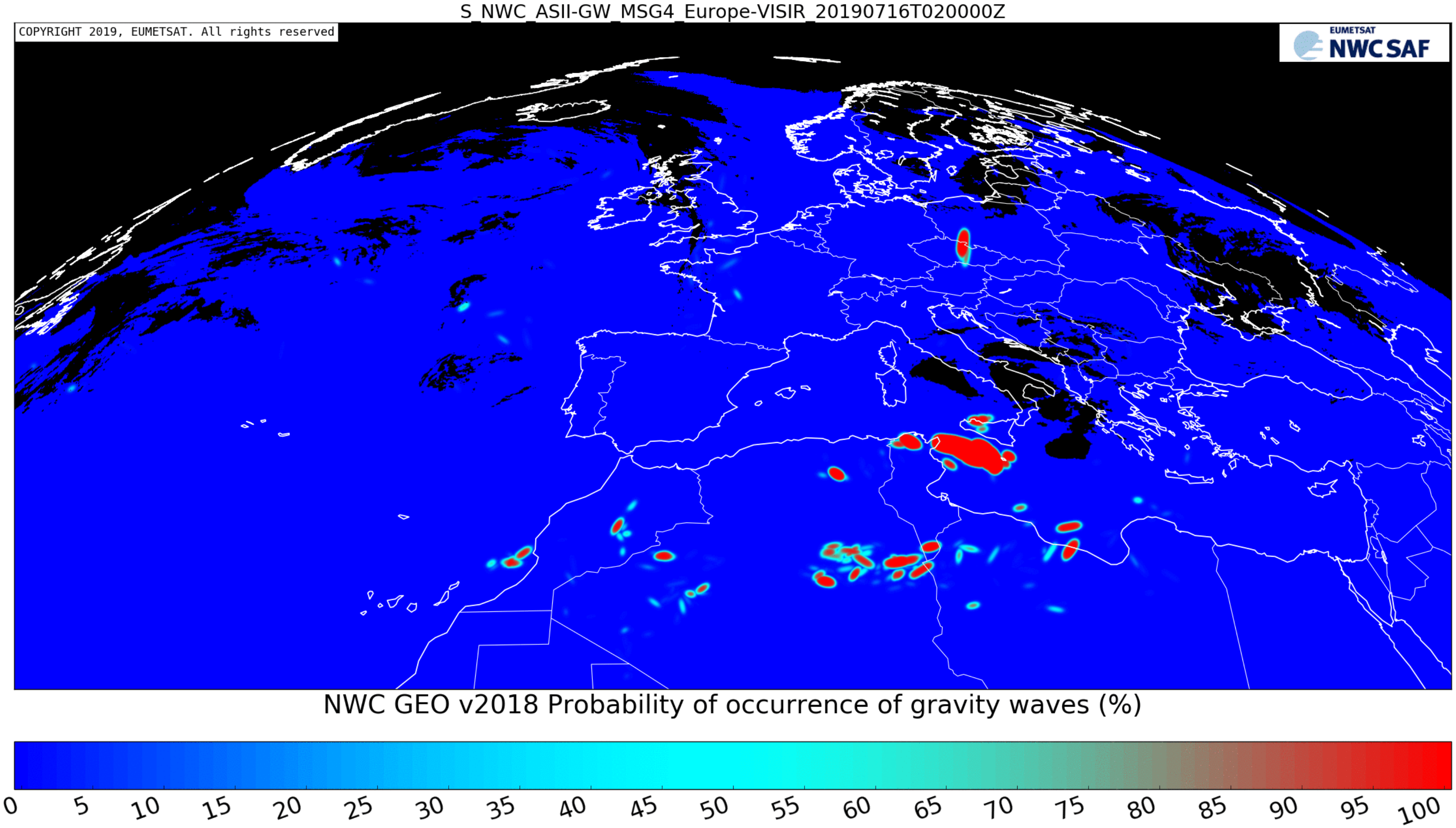

ZAMG
Zentralanstalt für Meteorologie und Geodynamik

S_NWC_ASII-GW_MSG4_Europe-VISIR_20190716T021500Z

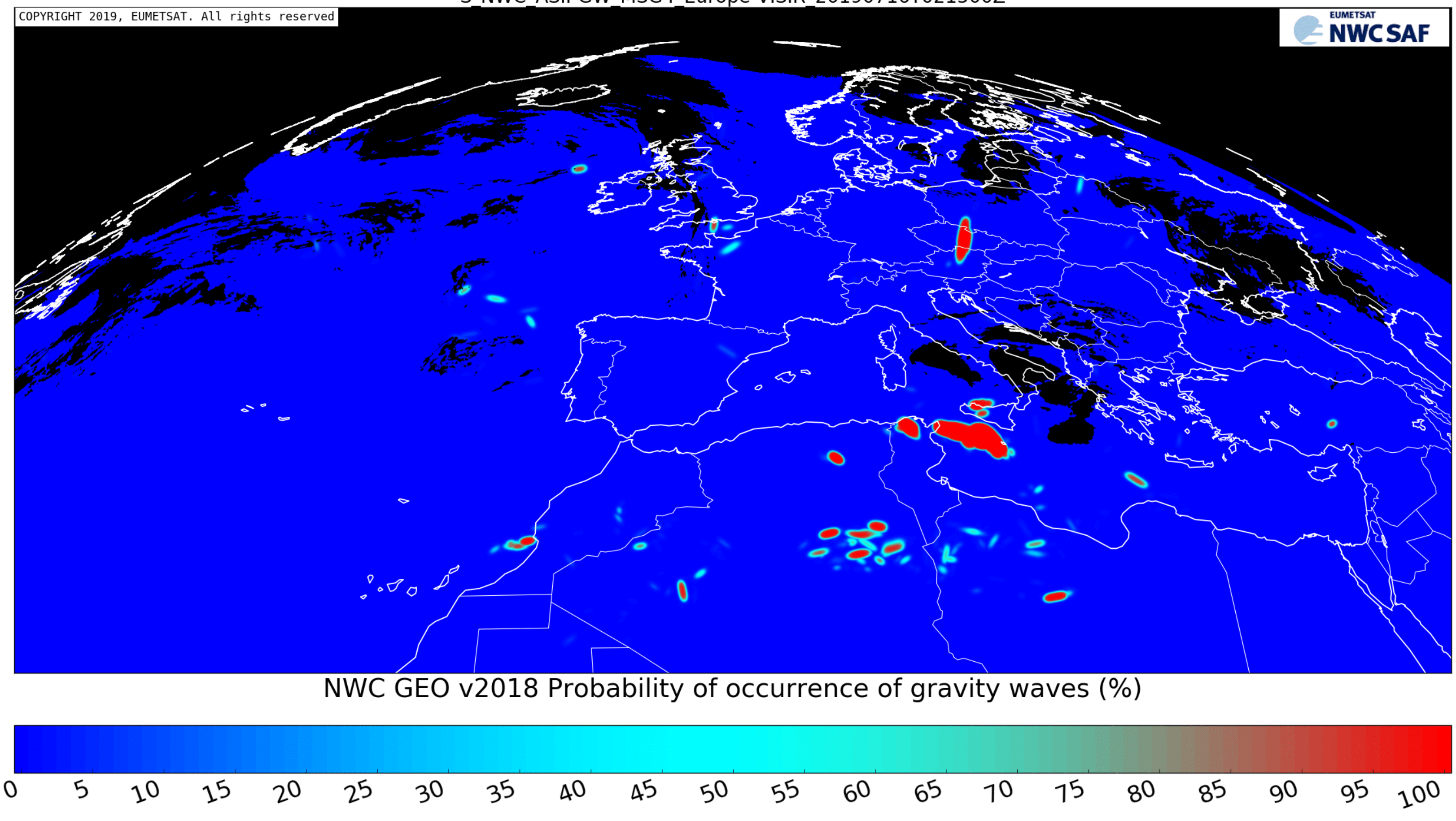

NWC GEO v2018 Probability of occurrence of gravity waves (%)

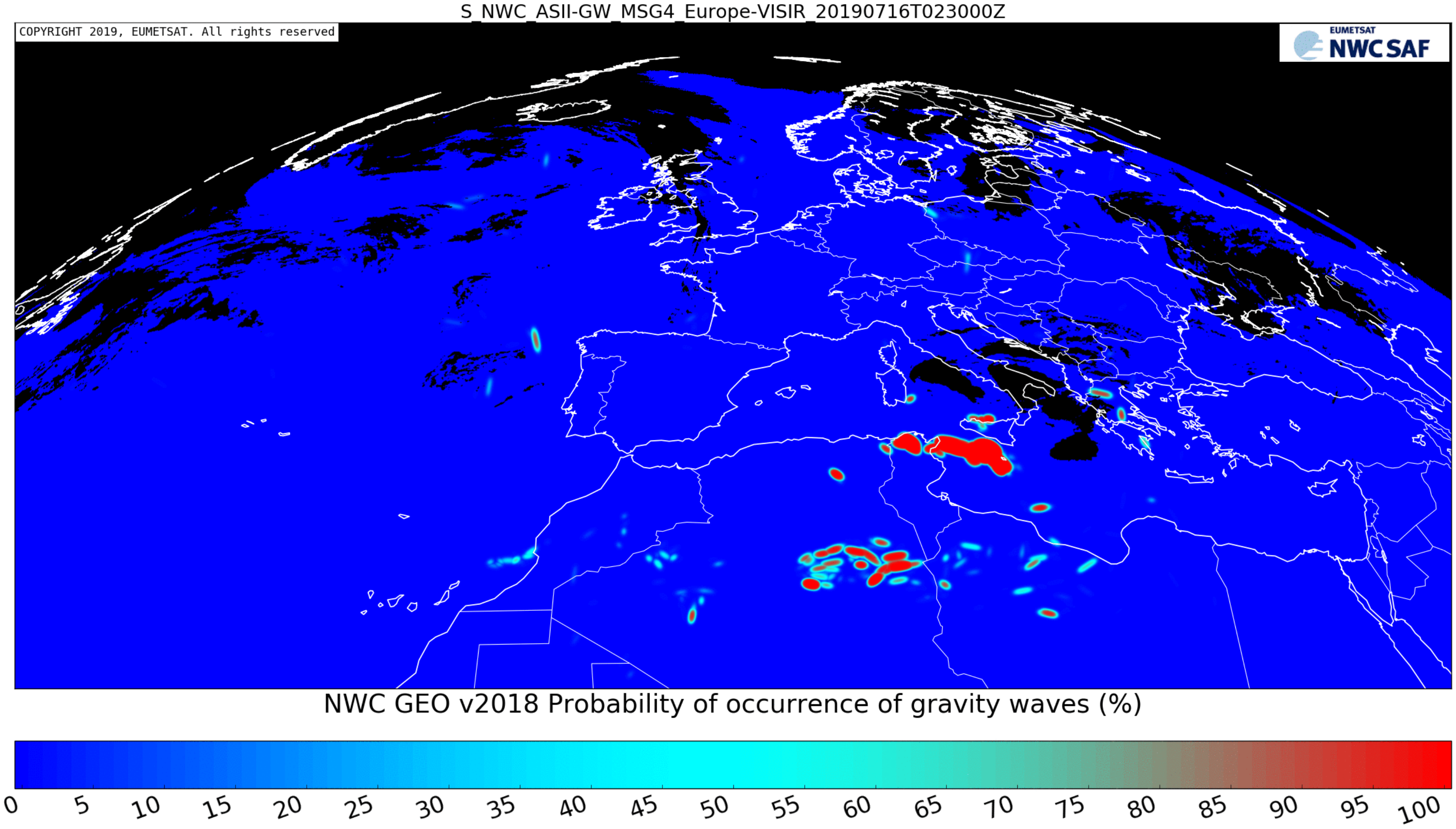
S_NWC_ASII-GW_MSG4_Europe-VISIR_20190716T023000Z
COPYRIGHT 2019, EUMETSAT. All rights reserved
EUMETSAT
NWC SAF
NWC GEO v2018 Probability of occurrence of gravity waves (%)
0
5
10
15
20
25
30
35
40
45
50
55
60
65
70
75
80
85
90
95
100

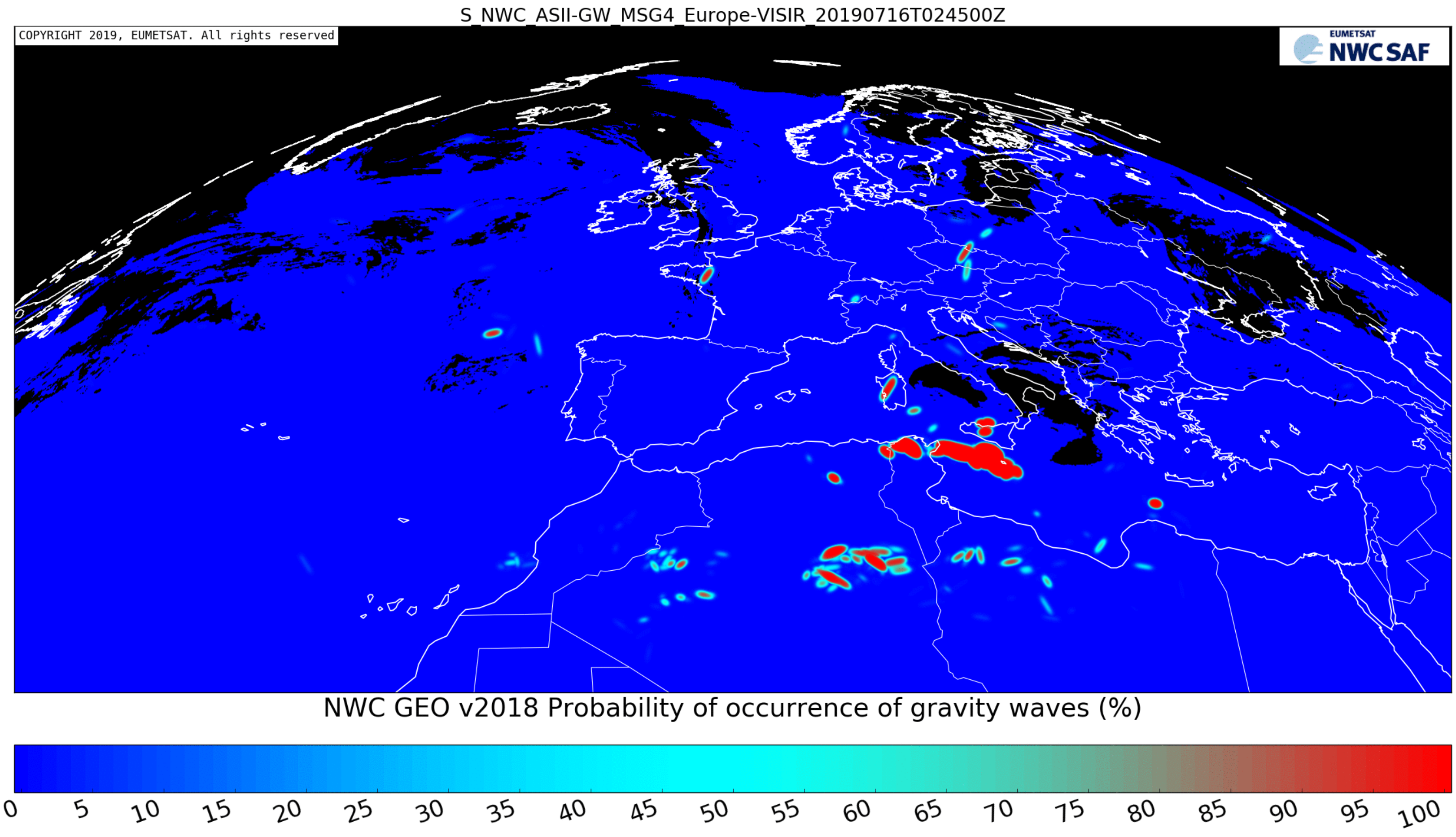

ZAMG
Zentralanstalt für Meteorologie und Geodynamik

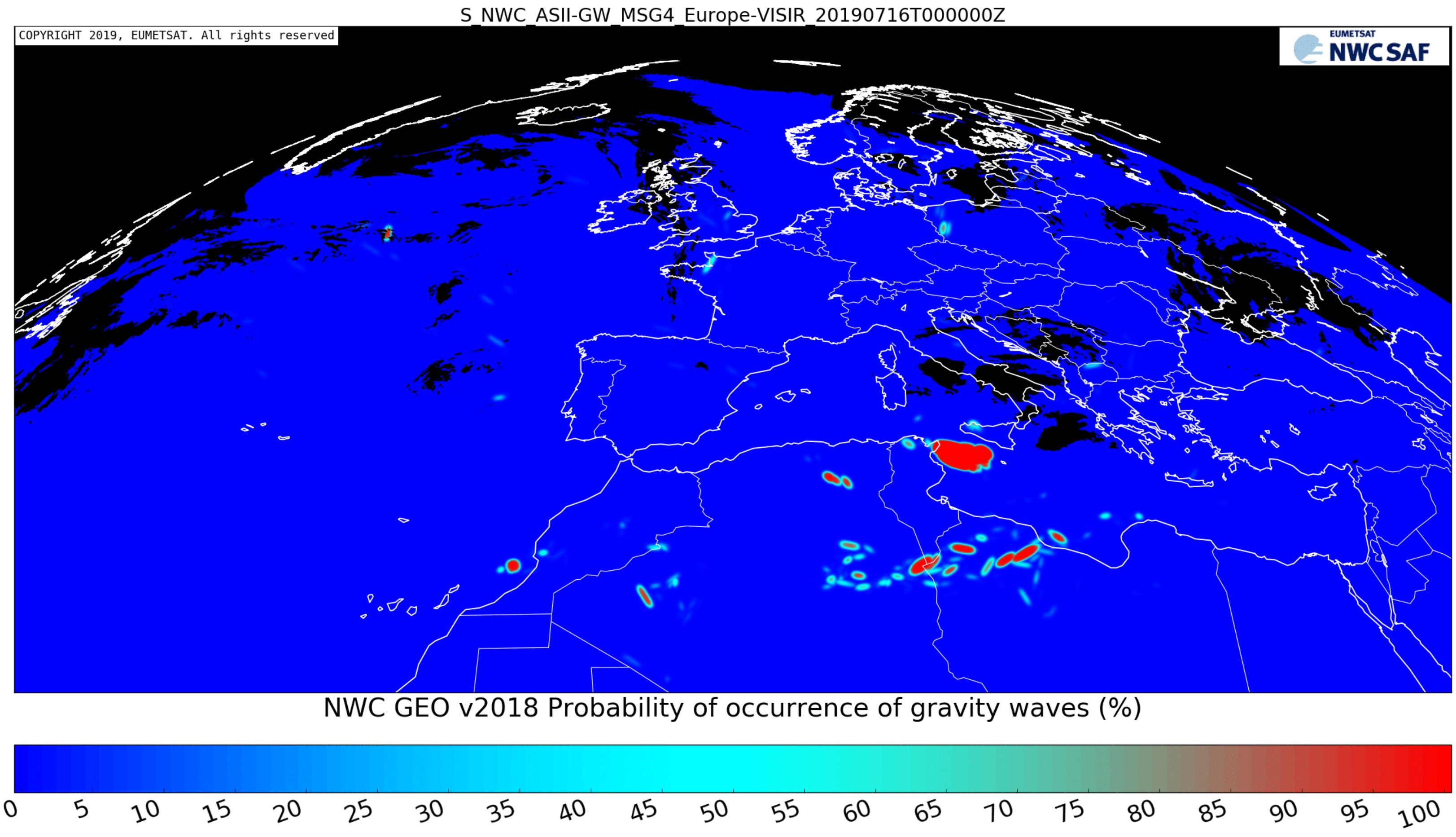

ZAMG
Zentralanstalt für Meteorologie und Geodynamik

S_NWC_ASII-GW_MSG4_Europe-VISIR_20190716T030000Z

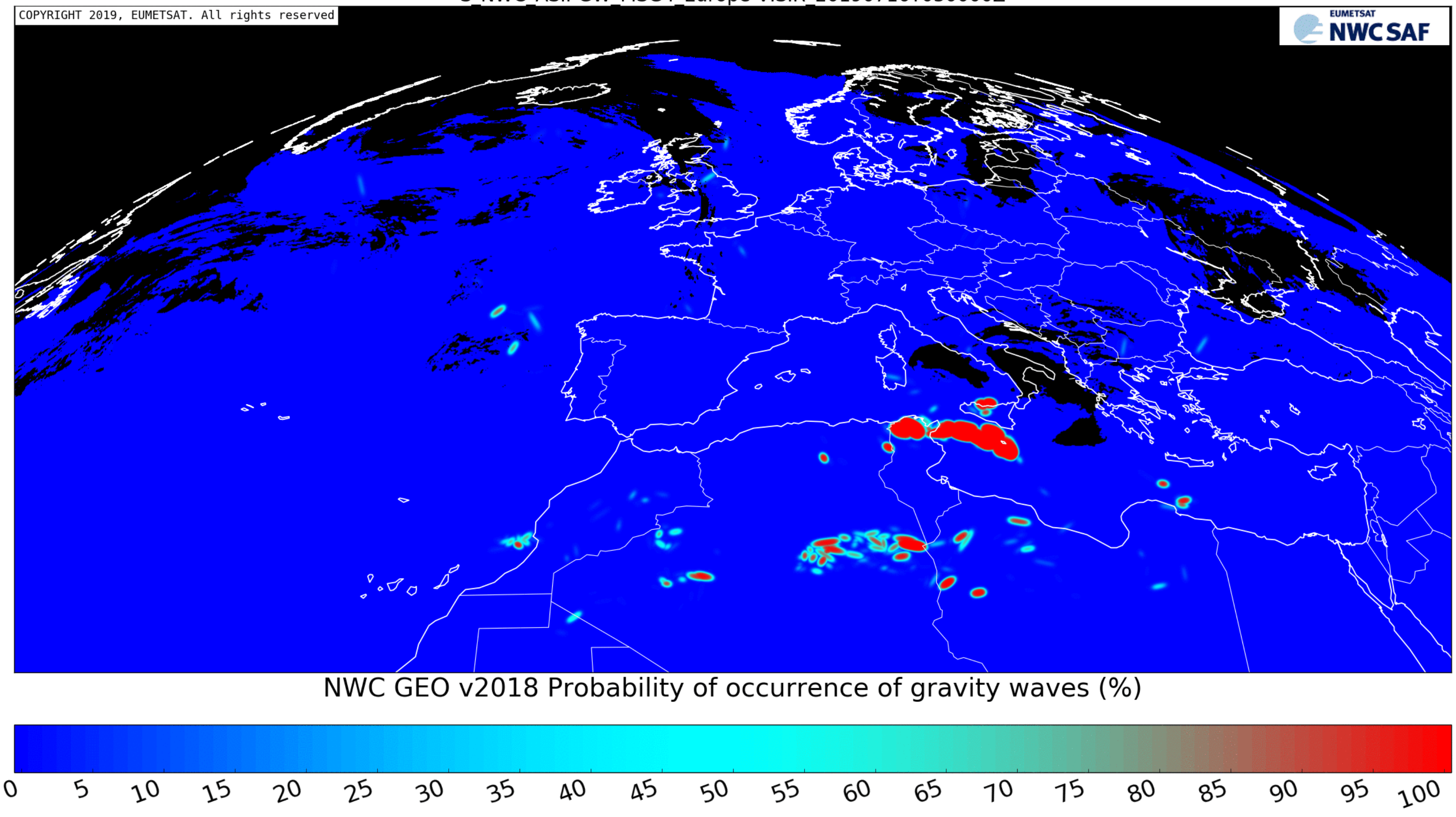

NWC GEO v2018 Probability of occurrence of gravity waves (%)

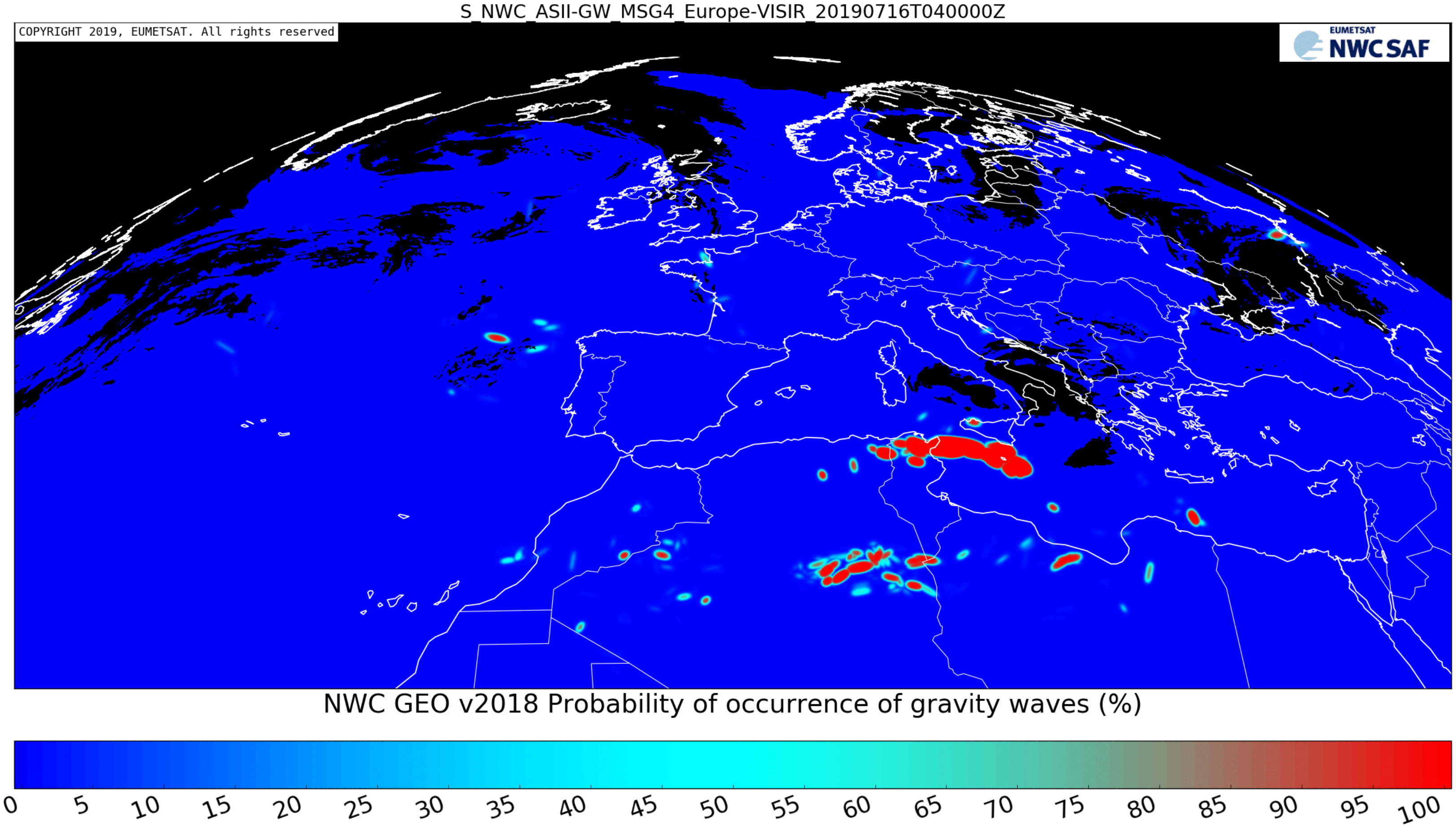
S_NWC_ASII-GW_MSG4_Europe-VISIR_20190716T040000Z
COPYRIGHT 2019, EUMETSAT. All rights reserved
EUMETSAT
NWC SAF
NWC GEO v2018 Probability of occurrence of gravity waves (%)
0
5
10
15
20
25
30
35
40
45
50
55
60
65
70
75
80
85
90
95
100

S_NWC_ASII-GW_MSG4_Europe-VISIR_20190716T041500Z

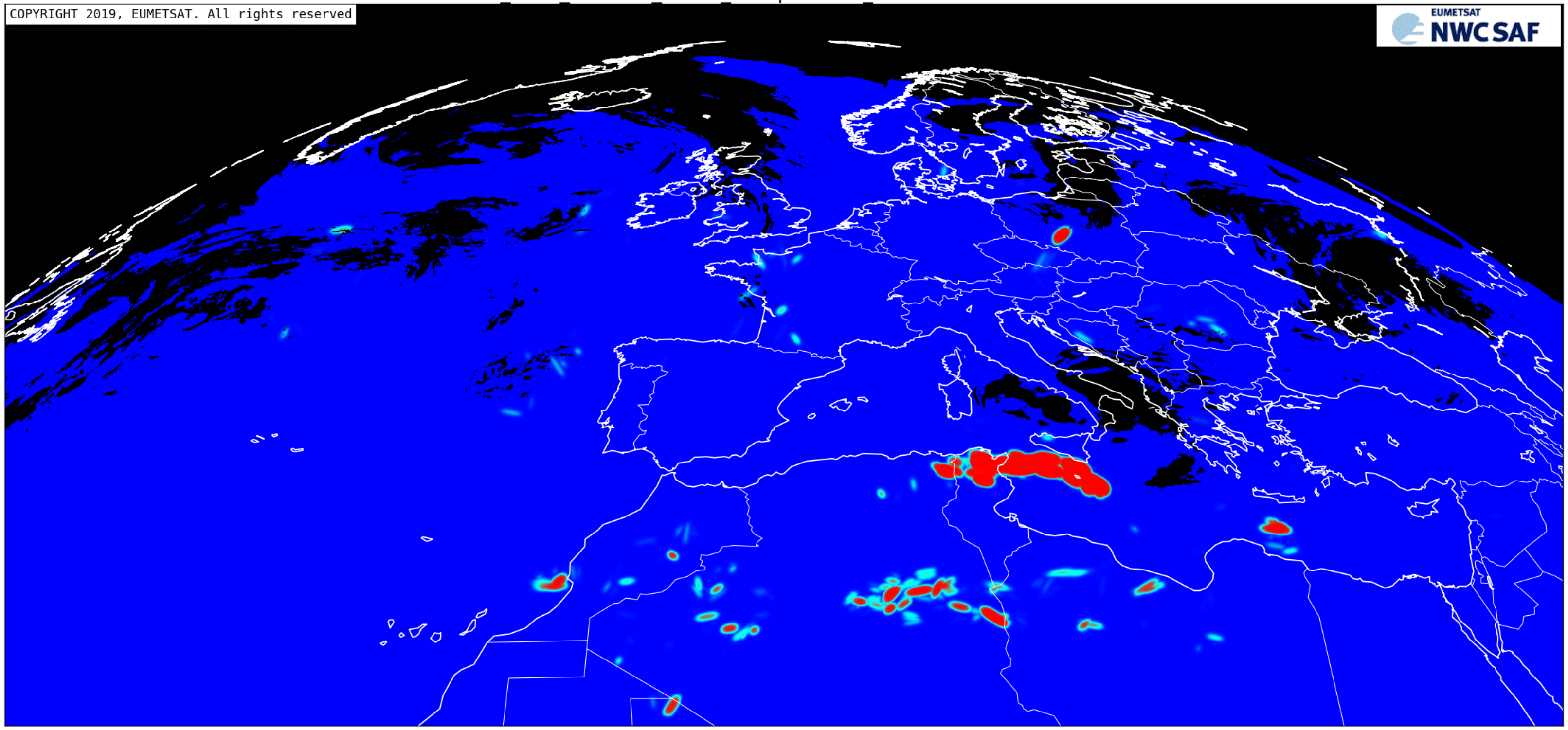

NWC GEO v2018 Probability of occurrence of gravity waves (%)

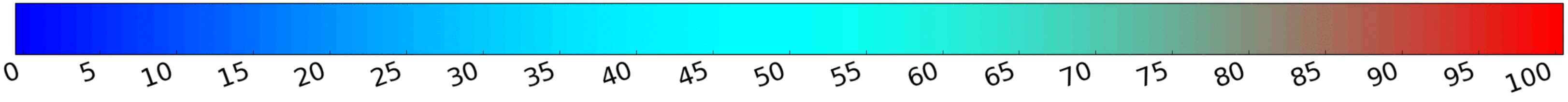

S_NWC_ASII-GW_MSG4_Europe-VISIR_20190716T043000Z

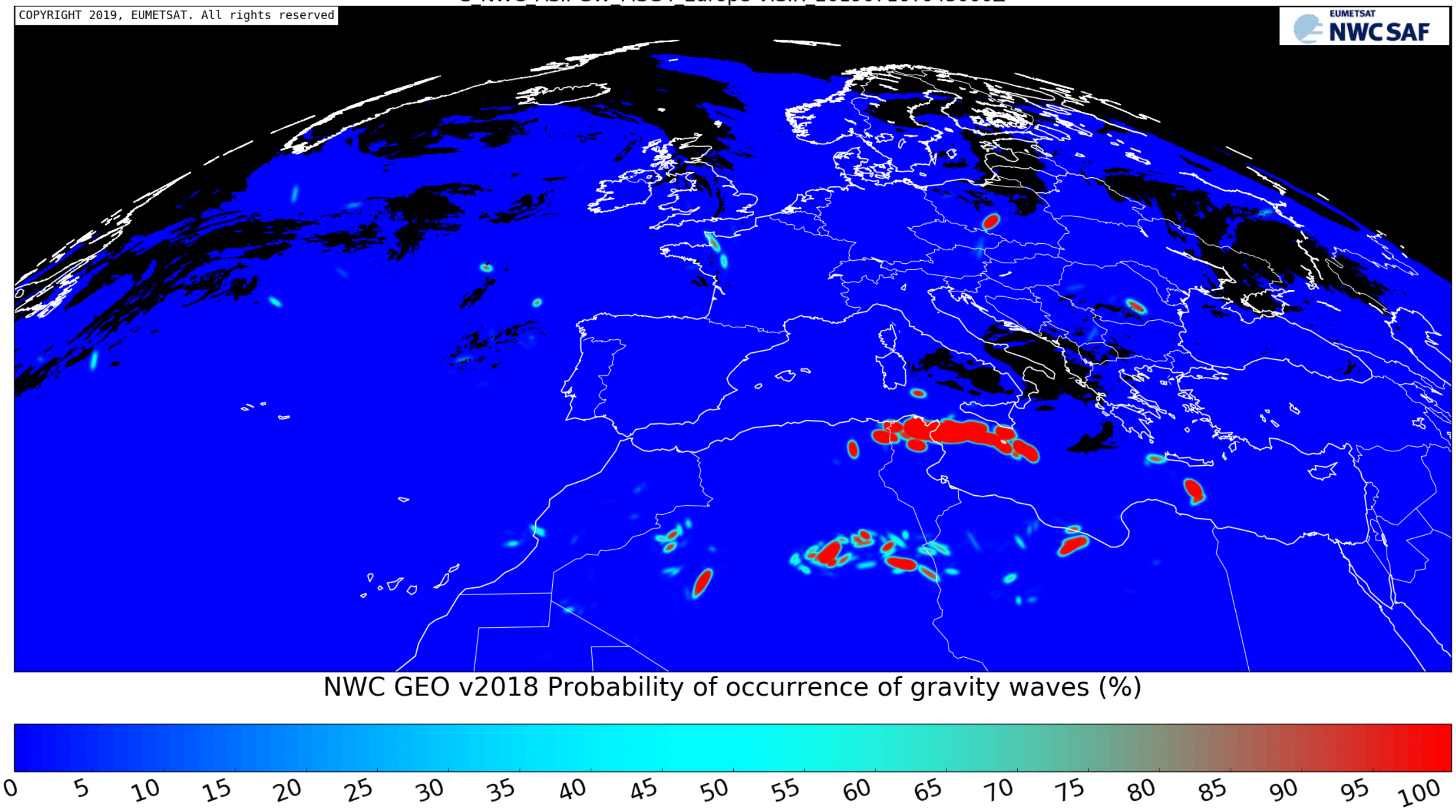

ZAMG Zentralanstalt für Meteorologie und Geodynamik

S_NWC_ASII-GW_MSG4_Europe-VISIR_20190716T044500Z

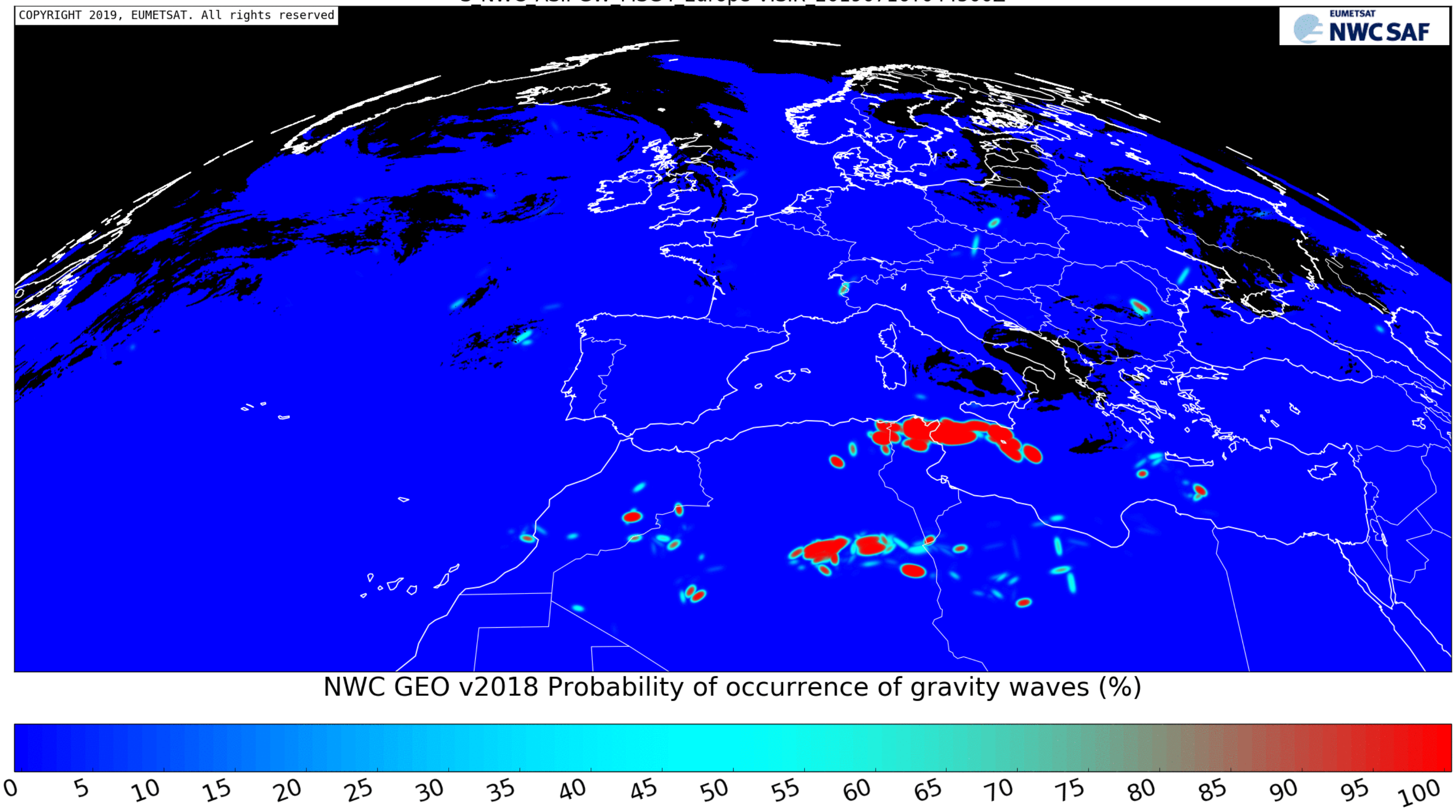

ZAMG
Zentralanstalt für Meteorologie und Geodynamik

WV7.3 chosen because marine Stratocumulus is less disturbing…

…whereas the algorithm does not appreciate patterns in HRVIS such as this one, and yields strong false-alarm signals:

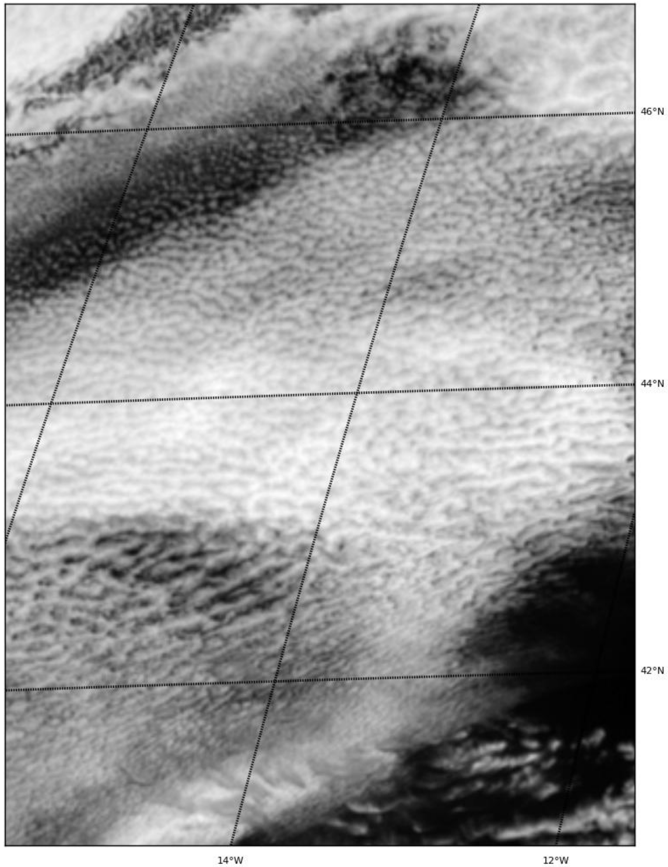

ZAMG
Zentralanstalt für Meteorologie und Geodynamik

Anticipated status at vMTG 2021+

- Technically capable of handling MTG
- Faster code, offset by 10-minute interval and higher number of pixels
- Algorithmic enhancement exploiting the information about the prevailing texture direction (i.e. the one with the highest Gabor filter response; Jann, 2019) →
  - Reduced risk of false alarms
  - Better perspectives to apply the same algorithm to IR imagery.

Status in a farther future

- Temporal continuity flagged (even exploited/integrated?)
- Parameter setting fine-tuned (even user-configurable?)

(e.g., Piani et al. 2000; Lane et al. 2001; Lane and Reeder 2001; Piani and Durran 2001; Beres et al. 2002) explicitly resolved the generation of gravity waves by deep convection, their model resolutions were too coarse (~1 km) to resolve turbulence-causing instabilities outside the clouds. The gravity waves generated in such models typically possess horizontal scales of approximately 10 km upward, which are too large to significantly affect aircraft. Some instability, such as wave breaking, is required to cause the cascade of energy down to the appropriate

!!??

(Wimmers and Feltz 2010). Verification using GOES WV imagery and automated aircraft Eddy Dissipation Rate (EDR) data was completed from Nov 2005 to Dec 2007. An accuracy of 53% for detection of moderate or greater CAT was achieved (the product requirement is at least 50%). The Tropopause Folding Turbulence Product (TFTP) is planned for future implementation with the GOES-R series.

4.4.2 Mountain waves

When moderate to strong winds blow across moun-

over 1964). The wavelength of the clouds is proportional to the wind speed and instability (Fritz 1965). Wavelengths have been observed to increase during the day as diurnal heating proceeds. The longer wavelengths (observable in GOES IR imagery) are more likely to be associated with significant low-level turbulence than the shorter wavelengths (Ellrod 1985). Figure 7 shows mountain waves in the Japanese Himiwari AHI and Multi-Transport Satellite (MTSAT) WV images on 7 July 2015. Their detection was made possible by the higher resolution (2 km) of the AHI WV band.

ZAMG Zentralanstalt für Meteorologie und Geodynamik

References

Jann, A. (2017): Detection of gravity waves in Meteosat imagery by grating cell operators. *Eur. J. Remote Sens.*, **50,** 509-516.

Jann, A. (2019): Objective detection of stripe patterns in satellite imagery caused by gravity waves: Lessons learnt from the southern hemisphere. *Trans. R. Soc. S. Afr.*, **74,** 163-172.

Keller, T.L., Trier, S.B., Hall, W.D., Sharman, R., Xu, M., & Liu, Y. (2015): Lee waves associated with a commercial jetliner accident at Denver International Airport. *J. Appl. Met. Clim.,* **54,** 1373-1392.

Petkov, N., & Kruizinga, P. (1997): Computational models of visual neurons specialised in the detection of periodic and aperiodic oriented visual stimuli: bar and grating cells. *Biol. Cybern.,* **76,** 83-96.

Wimmers, A., Griffin, S., Gerth, J., Bachmeier, S., & Lindstrom, S. (2018): Observations of gravity waves with high-pass filtering in the new generation of geostationary imagers and their relation to aircraft Turbulence. *Wea. Forecasting*, **33,** 139-144.

ZAMG
Zentralanstalt für Meteorologie und Geodynamik

THANK YOU FOR YOUR ATTENTION!

Dr. Alexander Jann
Section Head, NWP/Remote Sensing
Division "Data, Methods, Modeling"
Zentralanstalt für Meteorologie und Geodynamik
Hohe Warte 38
A-1190 Vienna
AUSTRIA
E-Mail: Alexander.Jann@zamg.ac.at
Tel.: +43 1 / 36 0 26 / 2316

ZAMG
Zentralanstalt für Meteorologie und Geodynamik